Received: 10 May 2022 | Revised: 6 July 2022 | Accepted: 19 July 2022

DOI: 10.1111/pce.14402

ORIGINAL ARTICLE

Plant, Cell & Environment | PC&E | WILEY

# Constitutive expression of *JASMONATE RESISTANT 1* induces molecular changes that prime the plants to better withstand drought

Sakil Mahmud[1,2] | Chhana Ullah[3] | Annika Kortz[4] | Sabarna Bhattacharyya[1] | Peng Yu[4,5] | Jonathan Gershenzon[3] | Ute C. Vothknecht[1]

[1]Plant Cell Biology, Institute of Cellular and Moleculara Botany, University of Bonn, Bonn, Germany

[2]Department of Biochemistry and Molecular Biology, Bangladesh Agricultural University, Mymensingh, Bangladesh

[3]Department of Biochemistry, Max Planck Institute for Chemical Ecology, Jena, Germany

[4]Crop Functional Genomics, Institute of Crop Science and Resource Conservation, University of Bonn, Bonn, Germany

[5]Emmy Noether Group Root Functional Biology, Institute of Crop Science and Resource Conservation, University of Bonn, Bonn, Germany

**Correspondence**
Ute C. Vothknecht, Plant Cell Biology, IZMB, University of Bonn, 53115 Bonn, Germany.
Email: vothknecht@uni-bonn.de

**Funding information**
Deutsche Forschungsgemeinschaft; Deutscher Akademischer Austauschdienst

## Abstract

In this study, we investigated *Arabidopsis thaliana* plants with altered levels of the enzyme *JASMONATE RESISTANT 1* (*JAR1*), which converts jasmonic acid (JA) to jasmonoyl-L-isoleucine (JA-Ile). Analysis of a newly generated overexpression line (35S::JAR1) revealed that constitutively increased JA-Ile production in 35S::JAR1 alters plant development, resulting in stunted growth and delayed flowering. Under drought-stress conditions, 35S::JAR1 plants showed reduced wilting and recovered better from desiccation than the wild type. By contrast, *jar1-11* plants with a strong reduction in JA-Ile content were hypersensitive to drought. RNA-sequencing analysis and hormonal profiling of plants under normal and drought conditions provided insights into the molecular reprogramming caused by the alteration in JA-Ile content. Especially 35S::JAR1 plants displayed changes in expression of developmental genes related to growth and flowering. Further transcriptional differences pertained to drought-related adaptive systems, including stomatal density and aperture, but also reactive oxygen species production and detoxification. Analysis of wild type and *jar1-11* plants carrying the roGFP-Orp1 sensor support a role of JA-Ile in the alleviation of methyl viologen-induced $H_2O_2$ production. Our data substantiate a role of JA-Ile in abiotic stress response and suggest that JAR1-mediated increase in JA-Ile content primes *Arabidopsis* towards improved drought stress tolerance.

**KEYWORDS**
JA-Ile, jasmonic acid, phytohormones, plant development, RNA-seq, ROS

## 1 | INTRODUCTION

Jasmonic acid (JA) and its derivatives, collectively known as jasmonates, are phytohormones involved in the regulation of plant growth, development and stress responses (for recent reviews, see Koo, 2018; Wasternack & Song, 2017). In the octadecanoid pathway, jasmonate biosynthesis is initiated from α-linolenic acid released from plastidial galactolipids through different lipoxygenases (13-LOXs) (Bell et al., 1995). Subsequently, ALLENE OXIDE SYNTHASE (AOS) and ALLENE OXIDE CYCLASES generate the first committed

precursor, 12-oxo-phytodienoic acid (*cis*-OPDA), which in peroxisomes is converted into JA by OPDA REDUCTASE 3 (OPR3) and β-oxidation. In the cytosol, JA is modified or conjugated to different derivatives, including the most bioactive form jasmonoyl-L-isoleucine (JA-Ile) (Koo, 2018; Wasternack & Song, 2017). JA-Ile content seems to be tightly controlled via different regulatory loops, including potential autoregulation of jasmonate synthesis (Hickman et al., 2017). Moreover, catabolic derivatives of JA and JA-Ile might play a role in maintaining jasmonate homoeostasis.

JASMONATE RESISTANT 1 (JAR1), a member of the GH3 family enzymes, holds a key position in jasmonate biosynthesis, because it catalyses the formation of JA-Ile from JA (Staswick & Tiryaki, 2004). JA-Ile can form a complex with the F-box protein CORONATINE INSENSITIVE 1 (COI1), various members of the transcriptional repressor JASMONATE ZIM-domain family (JAZ) and other components to form the $SCF^{COI1}$ complex (Koo, 2018; Wasternack & Song, 2017). Below a certain threshold level of JA-Ile, JAZ proteins interact with various transcription factors (TFs) that act as activators or repressors and ultimately regulate hundreds of genes. Accumulation of JA-Ile and formation of the $SCF^{COI1}$ complex targets the JAZ proteins for degradation through the 26S proteasome, thus releasing suppression of jasmonate responsive genes. The bHLH-type TF MYC2 is considered a master regulator of jasmonate signalling (Dombrecht et al., 2007). Induced by JA-Ile, MYC2 regulates the transcription of jasmonate-responsive genes such as *VEGETATIVE STORAGE PROTEINS* (*VSP1* and *VSP2*), shown to participate in plant development and defence (Devoto et al., 2005; Wasternack & Song, 2017). MYC2 also plays a role in terminating the jasmonate response via a negative feedback mechanism (Liu et al., 2019).

Drought is considered one of the major abiotic stresses that negatively affect plant growth and development (Yang et al., 2010). In *Arabidopsis*, exogenous MeJA application was shown to induce drought-responsive genes, whereas, vice versa, the exposure to drought induces jasmonate biosynthesis leading to JA-Ile accumulation (de Ollas et al., 2015a, 2015b; Harb et al., 2010; Zander et al., 2020). This relationship between jasmonate and drought stress was also reported for several crops (Creelman & Mullet, 1995; Du et al., 2013; Gao et al., 2004; Tayyab et al., 2020; Wang et al., 2021). Moreover, Marquis et al. (2022) showed recently that an *Arabidopsis* mutant in the *JASMONATE OXIDASE 2* (*JAO2*) gene locus, which is affected in jasmonate homeostasis, was more resistance to drought. Its drought resistant phenotype was dependent on JA-Ile signalling. The *jao2* mutant plants showed changes in the expression of defence-related genes already in unchallenged mutant leaves and also in the formation of defence-related metabolites. However, the allocation of metabolic resources to synthesize plant defence compounds is often associated with reduced growth and biomass accumulation (Züst & Agrawal, 2017).

Tolerance mechanisms to drought comprise a wide range of cellular processes. Among other things, reactive oxygen species (ROS) production is a common reaction to drought stress (Noctor et al., 2014). To cope with oxidative damage, jasmonate signalling was found to be involved in activating antioxidant mechanisms, such as regulating the ascorbate-glutathione (GSH) cycle and synthesis of polyphenols (Dombrecht et al., 2007; Savchenko et al., 2019). At the same time, stress adaptation relies on the interplay of multiple signalling pathways to integrate different environmental and developmental signals. Abscisic acid (ABA) is the hormone most closely associated with drought and it was shown that JA-Ile and ABA signalling interact under water stress conditions (de Ollas et al., 2015a, 2015b).

In this study, we used *Arabidopsis* lines with altered *JAR1* expression to change the endogenous JA-Ile content. We could show that alteration in JA-Ile content affects plant growth even under non-stress conditions. Furthermore, a reduced JA-Ile content makes plants more susceptible to progressive drought, while constitutively increased JA-Ile content strongly alleviates the deleterious effects of drought, making plants less susceptible and more likely to recover. In depth analysis of RNA-sequencing (RNA-seq) data obtained under control and early drought conditions provided insight into the transcriptional reprogramming caused by the alteration in JA-Ile content. Based on these data, the connection between JAR1-dependent changes in gene expression and differences in *Arabidopsis* growth and drought response phenotypes are discussed.

## 2 | MATERIALS AND METHODS

### 2.1 | Plant materials and growth conditions

If not otherwise stated, experiments in this study were performed on *Arabidopsis thaliana* (ecotype Columbia; Col-0) plants or transgenic lines created in the Col-0 background (Supporting Information: Figure S1A). The T-DNA insertion lines *jar1-11* (SALK_034543) and *jar1-12* (SALK_011510) were obtained from NASC (RRID: SCR_004576) and plants homozygous for the T-DNA insertion were identified by PCR screening (Supporting Information: Figure S1B). Primers are listed in Supporting Information: Table S1. Plants were grown either in standard plant potting soil pretreated with Confidor WG 70 (Bayer Agrar) or on ½ Murashige and Skoog medium (½ MS medium; Duchefa Biochemie) with 1% (w/v) sucrose and 0.6% (w/v) phytagel (Sigma-Aldrich, Inc.). Plants grown on ½ MS were stratified for 2 days at 4°C in the dark. Plants were cultured in climatized growth chambers (equipped with Philips TLD 18 W of alternating 830/840 light colour temperature) at 22°C under long-day conditions (16 h light/8 h dark) with 100 µmol photons $m^{-2}$ $s^{-1}$.

### 2.2 | Generation of JAR1-YFP overexpression lines

To generate plants expressing JAR1.1 as a fusion protein with yellow fluorescent protein (YFP) under the control of the 35S promoter (35S::JAR1.1-YFP), the entire coding sequence of the *JAR1.1* variant was cloned into the pBIN19 vector (Datla et al., 1992) in frame with the *YFP* sequence using ApaI and NotI restriction sites. The resulting construct (Supporting Information: Figure S1C) was stably

transformed into Col-0 using the floral dip method. Three independent homozygous T-DNA insertion lines (35S::JAR1) were obtained each in the F3 generation. JAR1.1-YFP expression was confirmed through RT-qPCR (Figure 1a), confocal microscopy (Supporting Information: Figure S1D) and western blotting using an antibody against green fluorescent protein (GFP; Supporting Information: Figure S1E).

## 2.3 | Plant phenotyping

For analysis of soil-grown plants, seeds were directly planted in potting soil. Five days later, young seedlings were transplanted to fresh pots containing 100 g potting soil (either one or four seedlings per pot). This was denoted as Day 1. Plants were then grown for 18 days with regular watering using identical volumes of tap water. Afterward, plants were either watered normally or exposed to drought stress conditions by withholding watering for up to 14 days. During the drought-stress treatment, pot weights were measured regularly. The relative soil water content (SWC) calculated as {(pot weight at the time of measurement) − (empty pot weight)}/{(initial pot weight) − (empty pot weight)} × 100 was adjusted between plant lines to ensure a similar drought stress level. After SWC dropped to 10%, plants were rewatered with equal volumes of tap water and survival rates of plants were calculated after 24 h and 7 days. The positioning of all pots in the climate chamber was randomized throughout the experiments. Photographs were taken at regular intervals and corresponding whole rosette leaves were collected for biochemical and RNA-seq analyses on Day 32.

For root growth assays, plants were grown on ½ MS plates with and without the addition of 50 µM MeJA. The root length was measured on Day 14.

## 2.4 | Stomatal aperture, density and relative water content (RWC) measurements

Stomatal aperture diameters and density were measured from the 6th leaf of 21-day-old plants grown under control conditions by collecting the leaf epidermis as described previously (Hossain et al., 2011). The RWC of leaves was calculated according to Barrs and Weatherley (1962).

## 2.5 | In vivo redox imaging

In vivo redox imaging was performed on the leaves of 7–9-day-old seedlings as described in (Meyer et al., 2007) using a Leica SP8 lightning (Leica Mikrosysteme). After pre-incubation in imaging buffer (10 mM MES, 10 mM $MgCl_2$, 10 mM $CaCl_2$, 5 mM KCl, pH 5.8), seedlings were transferred into a perfusion chamber (QE-1, Warner Instruments) to allow the exchange to different treatment solutions under constant imaging. Pinhole was adjusted to 3. After each run, representative samples were calibrated with 10 mM dithiothreitol (DTT; ratio = 0.18) and 10 mM $H_2O_2$ (ratio = 1.20). Data were processed using the integrated LASX software (RRID:SCR_013673) with the 'quantify' mode and the ratiometric image of 405/488 nm was calculated based on a standardization using 10 mM DTT and 10 mM $H_2O_2$.

## 2.6 | Anthocyanin measurements

Anthocyanin content was measured by adding 300 µl extraction buffer (1% [v/v] HCl in MeOH) to 100 mg of liquid $N_2$ ground leaf tissue, mixed with 200 µl $H_2O$ and 500 µl chloroform, and placed overnight at 4°C. After centrifugation, supernatants were collected and re-extracted with 400 µl of 60% methanol, 1% HCl. The absorbance was taken at 530 nm (anthocyanin) and 657 nm (background), and anthocyanin content was expressed as (A530-A657) per gram fresh weight.

## 2.7 | Western blot analysis

For extraction of total proteins, 100 mg finely ground leaf tissues were mixed with 100 µl 4× sodium dodecyl sulfate–polyacrylamide gel electrophoresis (SDS-PAGE) solubilizing buffer, vortexed and then incubated at 96°C for 10min. After centrifugation for 10 min at 14,000*g*, proteins in the supernatant were separated on 10% SDS-PAGE gels and blotted onto nitrocellulose membranes. Western blot analysis was performed by a standard protocol using an antibody against GFP (α-GFP; Roche, Cat# 11814460001, RRID:AB_390913) and a secondary antibody coupled with alkaline phosphatase (ThermoFisher Scientific Cat# 31320, RRID:AB_228304).

## 2.8 | Phytohormone analysis

Flash-frozen whole rosette leaves from three plants per sample were ground to a fine powder in liquid $N_2$. Approximately 50 mg of each sample was extracted with 1 ml methanol containing 30 ng $D_6$-JA, 6 ng $D_6$-JA-Ile (HPC Standards GmbH) and 30 ng $D_6$-ABA (Santa Cruz Biotechnology) as internal standards. The extracts were vortexed vigorously for 4–5 s and incubated for 2 min at 25°C under constant agitation at 1500 r.p.m. in a heating block. After 5 min centrifugation at 13000*g* and 4°C, ~900 µl of the supernatant was transferred to fresh microcentrifuge tubes. The residual tissues were reextracted using 750 µl 100% methanol without standards. The supernatants (1650 µl in total) were completely dried under a flow of $N_2$ at 30°C and redissolved in 300 µl 100% methanol.

Phytohormone analysis was performed on an Agilent 1260 high-performance liquid chromatography system (Agilent Technologies) attached to a QTRAP 6500 tandem mass spectrometer (Sciex) equipped with a turbo spray ion source operated in the negative ionization mode (Ullah et al., 2019, 2022). The concentrations of

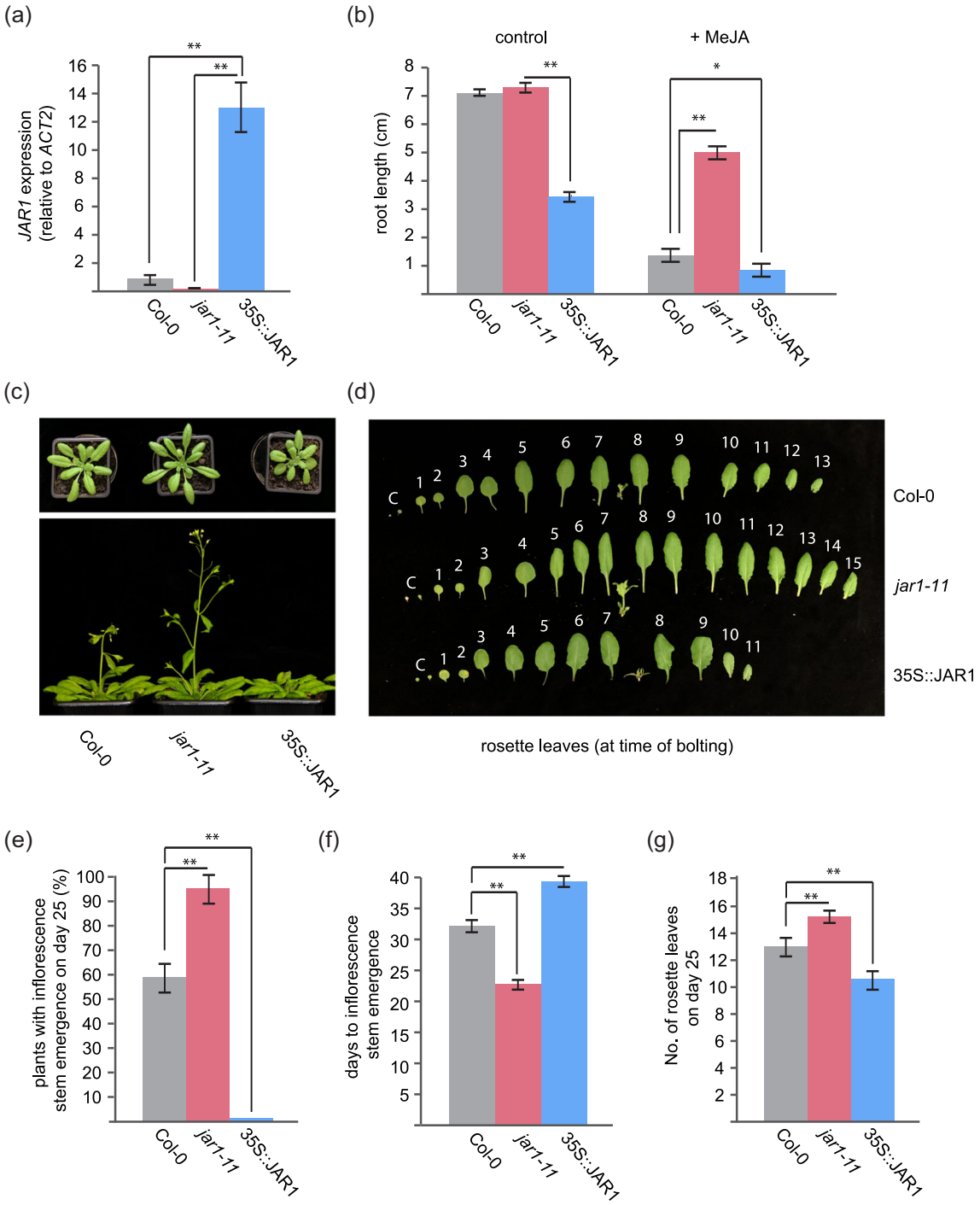


**FIGURE 1** Alteration in *JASMONATE RESISTANT 1* (*JAR1*) expression affects *Arabidopsis* leaf growth and flowering time. (a) *JAR1* transcript levels, relative to *ACT2*, in Col-0, *jar1-11* and 35S::JAR1 determined by RT-qPCR using rosette leaves of 25-day-old plants grown on soil. Data were analysed by one-way analysis of variance (ANOVA) (**$p < 0.01$) followed by multiple comparison analysis (Tukey's honest significant difference [HSD] test). Data represent means ± SE from three biological replicates ($n = 3$). (b) Root length of Col-0, *jar1-11* and 35S::JAR1 plants grown on ½ Murashige and Skoog medium (½ MS) medium with or without 50 µM MeJA (see also Supporting Information: Figure S2). Data were analysed by one-way ANOVA (*$p < 0.05$, **$p < 0.01$) followed by multiple comparison analysis (Tukey's HSD test). Data represent means ± SE from three biological replicates ($n = 3$), each containing >10 seedlings. (c) Representative photographs showing the growth phenotype of Col-0, *jar1-11* and 35S::JAR1 plants after 25 days (upper panel) and 32 days (lower panel). (d) Detached rosette leaves at the time of inflorescence stem emergence (~1 cm stem length). Leaves were detached at Day 32 (Col-0), Day 25 (*jar1-11*) and Day 40 (35S::JAR1). (e) Percentage of plants with emerged inflorescence stem of at least 1 cm at Day 25. Data represent means ± SE from five biological replicates ($n = 5$), each containing a minimum of five individual plants. (f) Average day by which inflorescence stems had emerged. Data represent means ± SE from five biological replicates ($n = 5$), each containing a minimum of five individual plants. (g) Rosette leaf numbers at Day 25. Data represent means ± SE from five biological replicates ($n = 5$), each containing a minimum of five individual plants. Data (e-g) were anlysed by one-way ANOVA (**$p < 0.01$) followed by multiple comparison analysis (Tukey's HSD test) [Color figure can be viewed at wileyonlinelibrary.com]

ABA, JA and JA-Ile were determined relative to the corresponding internal standards of $D_6$-ABA, $D_6$-JA and $D_6$-JA-Ile, respectively. Content of *cis*-OPDA was determined using $D_6$-JA, applying an experimental response factor (RF) of 1.0. Levels of 12-OH-JA-Ile and 12-COOH-JA-Ile were quantified relative to $D_6$-JA-Ile, applying an experimental RF of 1.0.

## 2.9 | RNA extraction, cDNA synthesis and RT-qPCR

Total RNA was extracted from the whole rosette leaves using the Quick-RNA Miniprep Kit (Zymo-Research). RNA quality and quantity were determined using a Nabi UV/Vis Nano Spectrophotometer (LTF Labortechnik). For RT-qPCR analysis, cDNA was prepared from 1 µg of messenger RNA (mRNA) with the RevertAid First Strand cDNA Synthesis Kit (Thermo Scientific, ThermoFisher Scientific). Gene expression was quantified using the Power SYBR Green PCR Master Mix in 48-well plates in a StepOne™ Real-Time PCR Thermocycler (Applied Biosystems, ThermoFisher Scientific) and the expression level was normalized to *ACTIN2* (*ACT2*) to express as relative quantity ($2^{-\Delta\Delta Ct}$). Primers used for RT-qPCR are listed in Supporting Information: Table S1.

## 2.10 | RNA-seq analysis

For each RNA-seq sample, the RNA extracted from three plants was pooled and the quality of RNA was checked by determining the RNA integrity number using a Tapestation 4200 (Agilent). For each line and experimental conditions, three independent pool samples were analysed. The library preparation and sequencing were performed by the NGS Core Facilities at the University of Bonn, Germany. Approximately 200 ng of RNA was used for library construction. Sequencing libraries were prepared using the QuantSeq 3′ mRNA-Seq Kit (Lexogen) and sequenced on an Illumina HiSeq. 2500 V4 platform with a read length of 1 × 50 bases. For each of the samples, three biological replicates were sequenced with an average sequencing depth of 10 million reads.

CLC Genomics Workbench v.12.03 (RRID:SCR_011853) was used to process the raw sequencing data. Quality control and trimming were performed on FASTQ files of the samples. Quality trimming was performed based on a quality score limit of 0.05 and a maximum number of two ambiguities. To map the additional JAR1 reads from the JAR1.1-YFP lines, an additional chromosome comprising the YFP sequence was added to the Araport 11 (Cheng et al., 2017) genome and the annotation file. The FASTQ samples were then mapped to the modified Araport 11 genome, while only classifying reads as mapped, which uniquely matched with ≥80% of their length and shared ≥90% identity with the reference genome. For the mapping to the gene models, reads had to match with ≥90% of their length and share ≥90% similarity with a maximum of one hit allowed. Further steps were completed using the R programming language (R Core Team, 2020). Gene Ontology (GO) term enrichment analysis was performed with the topGO package (RRID:SCR_014798). Additionally, transcripts per million (TPM) values were calculated based on the read counts. For individual genes, TPM values were compared by performing an analysis of variance (ANOVA) (RRID:SCR_002427) and a Tukey's honest significant difference (HSD) test with a confidence interval of 0.95 (Tukey & Hamner, 1949). Figures and plots were created using Venn Diagram, pheatmap, ggpubr and EnhancedVolcano included in the R package.

## 2.11 | Statistical analyses

Data were analysed statistically with ANOVA followed by multiple comparisons (Tukey's HSD test) in R. One-way ANOVA was used for all parameters except hormonal data where two-way ANOVA was applied. For additional experiments, a two-tailed *t*-test was used. Bar plots with error bars were generated in Microsoft Excel. Real-time monitoring of the roGFP2-Orp1 sensor was done using the XY-simple linear regression with 95% confidence level in GraphPad Prism v.9.0.0. (RRID:SCR_002798).

## 2.12 | Data availability

A list of accession numbers is provided in Supporting Information: Data Set_1. The RNA-seq data are deposited in the Gene Expression Omnibus (https://www.ncbi.nlm.nih.gov/geo/, RRID:SCR_005012) under the submission number GSE196602.

# 3 | RESULTS

To investigate the effect of JA-Ile on plant growth, we used the *Arabidopsis* T-DNA insertion line *jar1-11* (Supporting Information: Figure S1A and S1B) and a newly generated line expressing the YFP-tagged JAR1.1 splice variant under control of the 35S promoter (*35S::JAR1.1-YFP*) in a Col-0 background, which we refer to as 35S::JAR1 (Supporting Information: Figure S1C). RT-qPCR analysis of rosette leaves under normal growth conditions detected very low expression of *JAR1* transcripts in *jar1-11* (Figure 1a), confirming that it is a knockdown for *JAR1* (Suza & Staswick, 2008). By contrast, 35S::JAR1 plants showed strongly elevated expression of *JAR1* (Figure 1a). Fluorescence microscopy and western blot analysis with a GFP antibody furthermore confirmed the presence of high levels of JAR1.1-YFP protein in rosette leaves of the 35S::JAR1 line (Supporting Information: Figure S1D and S1E). Thus, these lines are a great resource to study the effects of varying internal JA-Ile levels on plant growth and stress responses.

### 3.1 | *JAR1* expression levels affect JA-Ile content and alters growth and flowering time

When tested on ½ MS medium, *jar1-11* plants grew similar as Col-0, whereas 35S::JAR1 plants exhibited a retarded growth phenotype (Figure 1b and Supporting Information: Figure S2). As was shown before, exogenous MeJA application strongly reduced root growth and shoot development in Col-0. MeJA can be taken up by the plant and in the presence of JAR1 is converted to JA-Ile. Consequently, the *jar1-11* plants were much less affected and developed quite well, whereas 35S::JAR1 plants were most severely affected by MeJA treatment. Upon extended growth on soil, *jar1-11* plants displayed a slightly larger rosette size than Col-0, whereas 35S::JAR1 plants showed slightly stunted growth with shorter and somewhat wider leaf blades (Figure 1c,d). Moreover, *jar1-11* plants were a few days ahead in bolting and flowering compared with Col-0, whereas 35S::JAR1 plants lagged behind by about 8–10 days (Figure 1c,e,f). The number of rosette leaves at the bolting stage also varied, with the highest in *jar1-11* (~14-16) and the lowest in 35S::JAR1 (~10–11) (Figure 1d,g). No significant differences were observed with other parameters related to reproductive success, such as the number and length of siliques, number of seeds per silique or germination rate (Supporting Information: Table S2).

Analysis of various jasmonates (Figure 2a–g, blue bars) in rosette leaves of the different plant lines grown on soil showed that JA-Ile content in Col-0 was low and in *jar1-11* plants virtually absent (Figure 2d). The 35S::JAR1 plants accumulated elevated levels of JA-Ile, indicating that substantial amounts of JA-Ile were synthesized and retained in the presence of constitutively elevated JAR1 protein. On the other hand, content of JA did not change much (Figure 2a). With regard to catabolic derivatives of JA and JA-Ile, 12-OH-JA, 12-OH-JA-Ile and 12-COOH-JA-Ile showed a substantial increase in the 35S::JAR1 plants (Figure 2b,e,f), suggesting that increased JA-Ile production in these plants also leads to an increased formation of catabolic products.

Plants of the *jar1-12* line, also containing significantly lower *JAR1* transcript levels, match the *jar1-11* phenotype of faster growth and early flowering, whereas two additional JAR1.1 overexpression lines support the stunted growth and late flowering observed in 35S::JAR1 (Supporting Information: Figure S3A and S3B). The early flowering phenotype seen in *jar1-11* is also found in other mutants related to jasmonate (Supporting Information: Figure S3C) where the pathway is blocked before JA-Ile production either at the synthesis of OPDA (*aos*) or JA (*opr3*). Together, our data indicate that changes in *JAR1* transcript levels alter JA-Ile content and that this alteration is the decisive factor for the observed difference in growth and development.

### 3.2 | Morphological differences between *jar1-11* and 35S::JAR1 are reflected in the expression of growth- and flowering-related genes

Global transcriptional differences in the rosette leaves of 32-day-old soil-grown plants were elucidated by RNA-seq analyses (Supporting Information: Data Set S1 and Figure S4). We found only four differentially expressed genes (DEGs) between *jar1-11* and Col-0 (Figure 3a and Supporting Information: Data Set S2), all of which were down-regulated. By contrast, we found 339 DEGs between 35S::JAR1 and Col-0 (Figure 3a,b and Supporting Information: Data Set S3) in line with the much stronger phenotypic difference observed between 35S::JAR1 and Col-0 compared with *jar1-11* under these growth conditions (Figure 1c).

The three genes down-regulated in *jar1-11* (but not 35S::JAR1) comprise *JAR1* itself, *AT1G22480* (a potential uclacyanin; cupredoxin superfamily protein) and the well-known jasmonate responsive *VSP1* gene (Figure 3c and Supporting Information: Data Set S2). Although the closely related *VSP2* showed only a slight, nonsignificant decrease in *jar1-11*, expression of both *VSP1* and *VSP2* was upregulated in 35S::JAR1 plants (Figure 3c). In line with the high levels of JA and JA-Ile derivatives, transcript levels of *IAA-LEUCINE RESISTANT (ILR)-LIKE GENE 6* (*ILL6*) and *JASMONATE-INDUCED OXYGENASES 3* (*JOX3*) were remarkably higher in 35S::JAR1. ILL6, a negative regulator of JA signalling, hydrolyses JA-Ile and 12-OH-JA-Ile to JA and 12-OH-JA, respectively (Bhosale et al., 2013; Widemann et al., 2013). JOX3 is involved in the oxidation of JA to 12-OH-JA (Smirnova et al., 2017).

Although it is described that JA-Ile accumulation releases transcriptional repression of *MYC2*, we found only a nonsignificant increase in *MYC2* expression in the 35S::JAR1 plants (Supporting Information: Data Set S4). This indicates that increase in JA-Ile alone is not sufficient to alter the expression of this postulated master regulator of jasmonate signalling. It also indicates that *VSP1* and *VSP2* expression can increase in a JA-Ile-dependent manner independent of MYC2. Expression of *MYC4*, a TF that was suggested to work additively to MYC2 in some jasmonate-mediated responses (Fernández-Calvo et al., 2011), was significantly decreased in 35S::JAR1 (Figure 3c). Interestingly, MYC4 was suggested to regulate the transcription of genes such as *GIF1*, a gene involved in the regulation of leaf expansion that was found to be increased in 35S::JAR1 (Supporting Information: Data Set S4). Furthermore, several of the DEGs upregulated in 35S::JAR1 as compared with Col-0 are involved in cell cycle control, for example, *SYP111* (*KNOLLE*), *FBL17*, *CYCA3;2* and *CYCB1;2* (Supporting Information: Data Set S4), and play a role in leaf growth and expansion (Vercruysse et al., 2020).

Although *jar1-11* plants showed early and 35S::JAR1 plants delayed flowering compared with Col-0 (Figure 1c), we found no variation in major photoperiod-related floral responsive genes such as *FT*, *LEAFY* or *APETALA2* (Kinoshita & Richter, 2020). However, a heat map shows enhancement of *FLOWERING LOCUS C* (*FLC*) expression in 35S::JAR1 (Figure 3d), a major player of the autonomous flowering-time pathway (Wu et al., 2020). Early flowering inhibition by FLC involves repression of *SOC1* (Michaels & Amasino, 2001), whose expression was decreased in 35S::JAR1, as was the expression of the early flowering inducers *MAF1* (Ratcliffe et al., 2001) and *SPL4* (Wu & Poethig, 2006). On the other hand, expression of *MYROSINASE BINDING PROTEIN 2* (*MBP2*; *F-ATMBP*), which is related to flowering regulation through the COI1 receptor (Capella et al., 2001), was enhanced (Figure 3D).

Overall, the results suggest that the higher JA-Ile level in 35S::JAR1 causes changes in the expression of growth and flowering-related genes

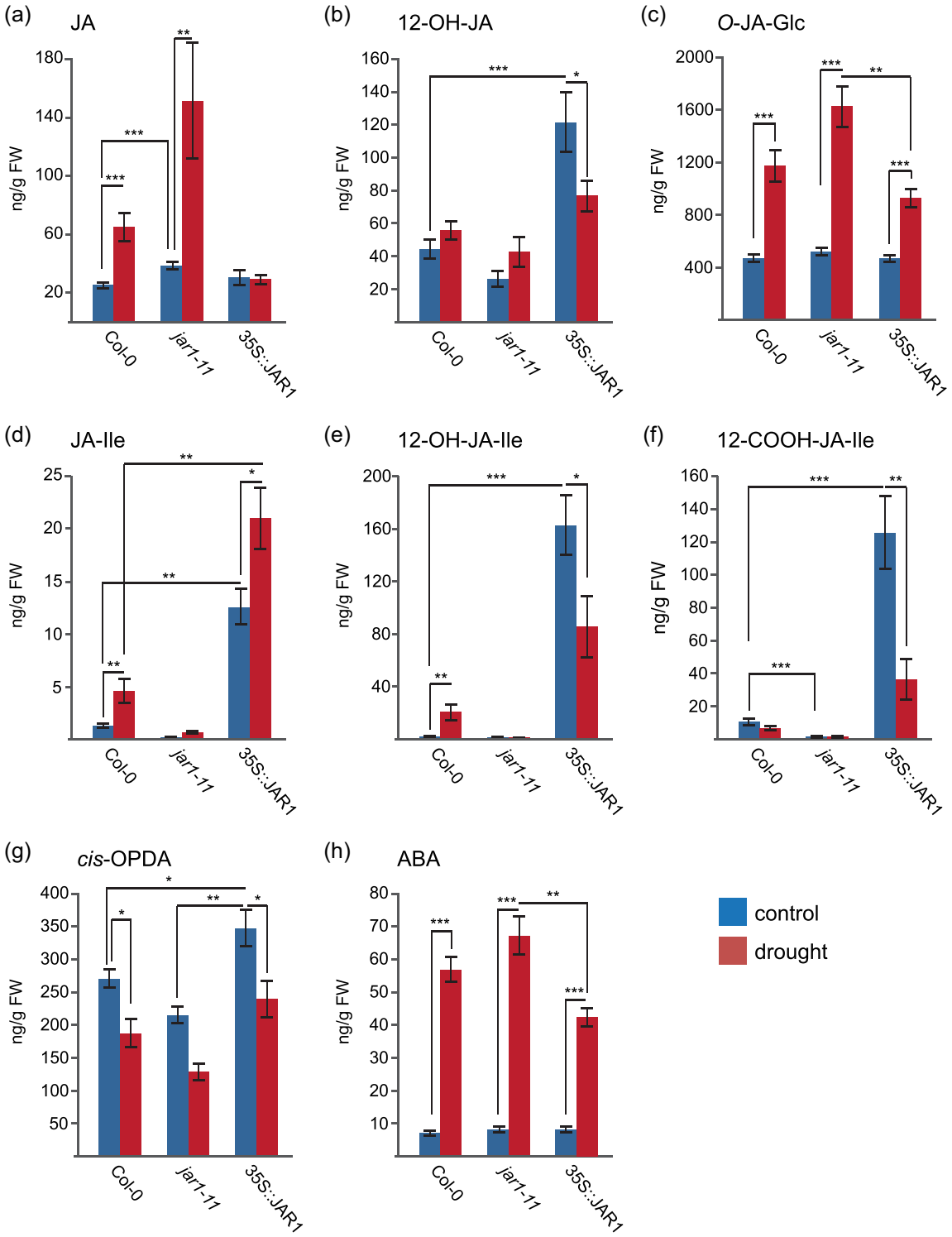


**FIGURE 2** *JASMONATE RESISTANT 1* (*JAR1*)-dependent changes in the contents of jasmonates and abscisic acid (ABA). The contents of different jasmonates (a–g) and ABA (h) were determined in rosette leaves of 32-day-old plants from wild type (Col-0), *jar1-11* and 35S::JAR1 grown under control and drought stress conditions. Compounds measured were jasmonic acid (JA), 12-hydroxy-jasmonic acid (12-OH-JA), 12-hydroxyl-jasmonoyl-glucoside (12-*O*-Glc-JA), jasmonoyl-L-isoleucine (JA-Ile), 12-hydroxy-jasmonoyl-isoleucine (12-OH-JA-Ile), 12-carboxy-jasmonoyl-isoleucine (12-COOH-JA-Ile), 12-oxo-phytodienoic acid (*cis*-OPDA) and ABA. Data represent means± SE from six replicates ($n = 6$), each containing pooled extracts from three plants. Data were analysed by two-way analysis of variance (ANOVA) (*$p < 0.05$, **$p < 0.01$, ***$p < 0.001$) followed by multiple comparison analysis (Tukey's honest significant difference [HSD] test). [Color figure can be viewed at wileyonlinelibrary.com]

resulting in rosettes with shorter but wider leaves and a delay in transition from vegetative to reproductive mode.

### 3.3 | *JAR1* expression levels affect drought tolerance of *Arabidopsis*

We next performed progressive drought experiments by withholding water from 18-day-old well-watered plants (Figure 4a). After 2 weeks of water withholding (Day 32), the first indications of drought effects occurred (Figure 4b and Supporting Information: Figure S5A). Hypersensitivity of *jar1-11* to drought became clearly visible at Day 36, with *jar1-11* plants displaying severe signs of wilting compared with Col-0. Three days later, both Col-0 and *jar1-11* plants had reached a state of unrecoverable wilting and re-watering at this stage resulted in 0% survival. By contrast, 35S::JAR1 plants displayed an extended drought tolerance and showed first signs of wilting only at Day 39, which could be fully recovered by re-watering (Figure 4b and Supporting Information: Figure S5A). In line with the visible effects, 35S::JAR1 plants retained about 80% RWC at Day 36, whereas the RWC of Col-0 and *jar1-11* plants dropped to 50% and 30%, respectively (Figure 4c). The drought-susceptible phenotype of *jar1-11* could also be confirmed in the *jar1-12* line (Supporting Information: Figure S5B).

To ensure that the better performance of 35S::JAR1 plants under drought was not a direct effect of the reduced biomass and thus lower water uptake from the soil, Col-0, *jar1-11* and 35S::JAR1 plants were grown together in the same pot. With four plants in the same size pot, drought effects were slightly more severe also in 35S::JAR1, but as before, the 35S::JAR1 plants showed lesser wilting and recovered after only 1 day of re-watering, with no recovery seen for Col-0 and *jar1-11* plants (Supporting Information: Figure S5C). In a separate drought stress experiment, Col-0 plants were treated with a foliar spray of MeJA on Day 11, before the start of water withholding (Day 18). Similar to 35S::JAR1, MeJA-treated Col-0 plants showed stunted growth together with better drought resistance and recovery (Supporting Information: Figure S5D).

At Day 32, already before the onset of any severe drought effects, JA-Ile content increased significantly in Col-0 and 35S::JAR1, confirming that the plants already experience water deficiency and react by inducing jasmonate biosynthesis (Figure 2d). By contrast, JA-Ile content remained virtually absent in *jar1-11* even under these conditions. However, JA content in *jar1-11* was strongly increased (Figure 2a), likely because jasmonate biosynthesis is induced but the

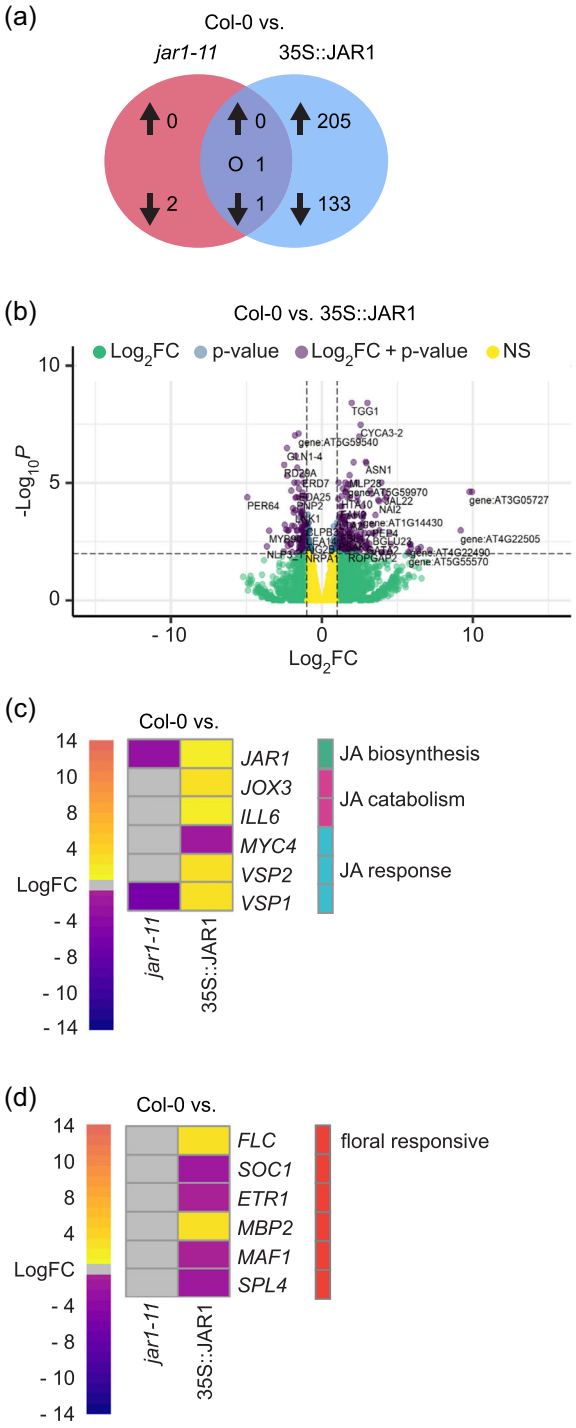


**FIGURE 3** *JASMONATE RESISTANT 1* (*JAR1*)-dependent changes in gene expression in rosette leaves under normal growth conditions. (a) Venn diagram showing differentially expressed genes (DEGs; DESeq, adjusted to false discovery rate (FDR) < 0.01 and |LogFC| ≥ 1) in *jar1-11* and 35S::JAR1 compared with Col-0 in 32-day-old plants under normal growth conditions. Arrows indicate up- and downregulation. 'O' indicates counter-regulated genes. (b) Volcano plot showing statistical significance ($\log_{10}P$) versus magnitude of change (LogFC) of DEGs between Col-0 and 35S::JAR1. Violet dots indicate genes that fit the DESeq criteria of FDR < 0.01 and |LogFC| ≥ 1, whereas green and blue dots represent DEGs that fit only LogFC or FDR, respectively. (c, d) Heat maps of genes involved in JA biosynthesis, catabolism and signalling response (c) or flowering responsive genes (c). Expression was compared between Col-0 and *jar1-11* or 35S::JAR1. Data were analysed using a cut-off of FDR < 0.05 and |LogFC| ≥ 0.5. [Color figure can be viewed at wileyonlinelibrary.com]

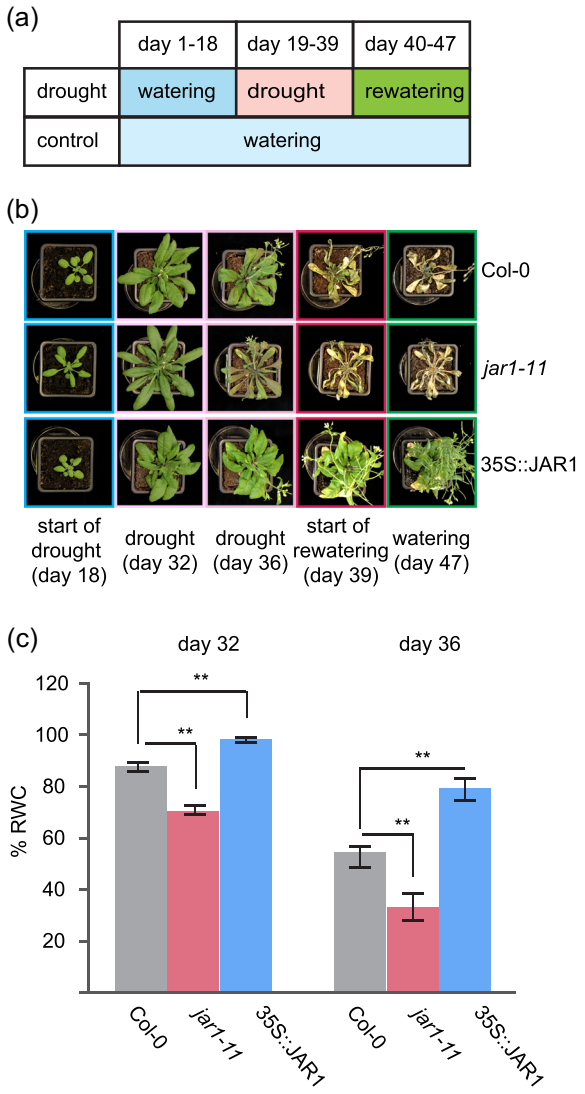


**FIGURE 4** Increased *JASMONATE RESISTANT 1* (*JAR1*) expression positively affects drought stress tolerance. (a) Schematic representation of the progressive drought stress experiment. Watering was stopped on Day 18. Drought exposed plants were watered again at Day 39. (b) Representative photographs showing plant phenotypes throughout the progressive drought stress experiment (see also Supporting Information: Figure S4A). (c) Leaf relative water content (% RWC) of drought-treated plants on Days 32 and 36. Data represent means ± SE from five biological replicates ($n = 5$), each containing five individual plants. Data were analysed by one-way analysis of variance (ANOVA) (**$p < 0.01$) followed by multiple comparison analysis (Tukey's honest significant difference [HSD] test). [Color figure can be viewed at wileyonlinelibrary.com]

pathway to JA-Ile is blocked. Content of the committed precursor *cis*-OPDA decreased in all lines under drought (Figure 2g) at levels in line with the formation of JA, JA-Ile and derivatives thereof. Especially *O*-JA-Glc levels, which were quite similar under control conditions, markedly increased in all lines upon drought (Figure 2c). Compared with Col-0, the increase was higher in *jar1-11* and lower in 35S::JAR1 (Figure 2C). Similarly, the contents of ABA, which did not differ statistically under control conditions, increased upon exposure to drought with the highest increase in *jar1-11* and lowest in the 35S::JAR1 plants (Figure 2h).

### 3.4 | JAR1-mediated JA-Ile formation regulates genes related to drought resistance and responses mechanisms

We also performed RNA-seq analysis on Day 32 in plants grown under drought conditions (Supporting Information: Figure S4 and Data Set S2). In Col-0, we identified 3401 DEGs (Figure 5a) between control and drought-treated plants. By comparison, *jar1-11* plants showed a much higher (6139) and 35S::JAR1 a lower number (2025) of DEGs. The higher number of DEGs observed in the *jar1-11* plants supports that already at this point they experience a higher level of drought stress even though plants of the different lines still looked similar.

A comparison of the RNA-seq data between the different plant lines under drought conditions revealed 2411 DEGs between Col-0 and *jar1-11* and 998 DEGs between Col-0 and 35S::JAR1 (Figure 5b and Supporting Information: Data Set S3). Of these, 391 DEGs were counter-regulated between *jar1-11* and 35S::JAR1. GO enrichment analysis confirmed a reciprocal trend between *jar1-11* and 35 S::JAR1 for a number of genes (Supporting Information: Data Set S5). Several of the genes involved in jasmonate biosynthesis upstream of *JAR1* showed a lower expression in *jar1-11* under drought compared with Col-0, whereas their expression was similar or higher than Col-0 in 35S::JAR1 plants (Figure 5c). A similar pattern was observed for the expression of the jasmonate-related TF *MYC2*, the jasmonate-dependent genes *VSP1* and *VSP2*, as well as most *JAZ* genes (Figure 5c). Remarkably, two of the *JAZ* genes show an opposite trend.

The majority of genes with decreased expression in *jar1-11* and increased expression in 35S::JAR1 were related to photosynthesis (Supporting Information: Data Set S5). On the other hand, the majority of genes with increased expression in *jar1-11* and decreased expression in 35S::JAR1 included various groups of genes responding to abiotic stresses and other hormones. Not surprisingly, genes known to be responsive to drought and ABA signalling were enriched in the upregulated gene sets of all three lines upon drought (Supporting Information: Data Set S3 and S4). However, compared with Col-0 and 35S::JAR1, *jar1-11* plants showed a stronger upregulation of several genes involved in the ABA signalling pathway (Figure 5c).

To further investigate the differential expression in response to drought compared with control conditions, we applied hierarchical clustering to all DEGs among Col-0, *jar1-11* and 35S::JAR1 (Supporting Information: Data Set S6). These clusters can be categorized into two sets, with the first set (Clusters 1-4) representing mechanisms to withstand drought stress effects (Figure 6). We found a decreased expression after drought stress in all lines in Clusters 1–4, albeit to a lesser extent in 35S::JAR1 compared with Col-0 and especially with *jar1-11*. Many genes in

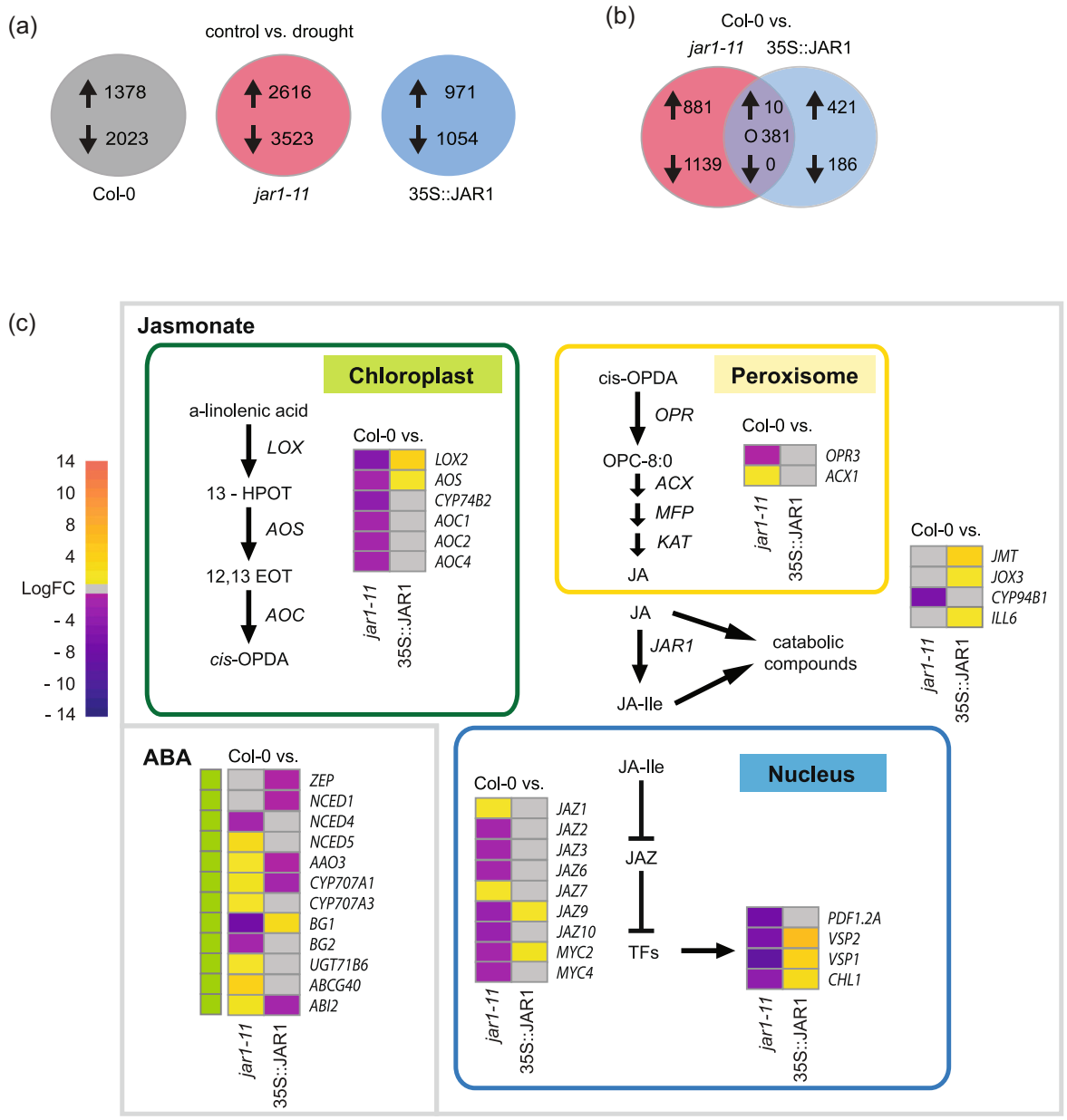


**FIGURE 5** *JASMONATE RESISTANT 1* (*JAR1*)-dependent changes in gene expression in rosette leaves under progressive drought. (a) Number of differentially expressed genes (DEGs; DESeq, adjusted $p < 0.01$ and $|\text{LogFC}| \geq 1$) between control and drought conditions in Col-0, *jar1-11* and 35S::JAR1. Arrows indicate up- and downregulation. (b) Venn diagram of DEGs (DESeq, adjusted $p < 0.01$ and $|\text{LogFC}| \geq 1$) in *jar1-11* and 35S::JAR1 compared with Col-0 under drought conditions. Arrows indicate up- and downregulation. 'O' indicates counter-regulated genes. (d) Heat maps of genes involved in jasmonate biosynthesis, catabolism and signalling response depicted by cell compartments, as well as abscisic acid (ABA) biosynthesis, catabolism and signalling response compared between Col-0 and either *jar1-11* or 35S::JAR1, all under drought conditions. Data were analysed using a cut-off of false discovery rate (FDR) < 0.05 and $|\text{LogFC}| \geq 0.5$. [Color figure can be viewed at wileyonlinelibrary.com]

Cluster 1 relate to water transport, whereas Clusters 2 and 4 clearly represent the detrimental effect of drought on the photosynthetic machinery. Genes related to growth regulation were affected on several levels from general regulation of growth (Cluster 1) to cell wall biosynthesis and remodelling (Cluster 3). Cytokinin response was also negatively affected by drought, especially in *jar-11*. By contrast, Cluster 5 comprises genes upregulated in all three lines with the highest upregulation in *jar1-11*. Many of these genes represent drought stress responses such as ABA-dependent and independent genes related to water deprivation.

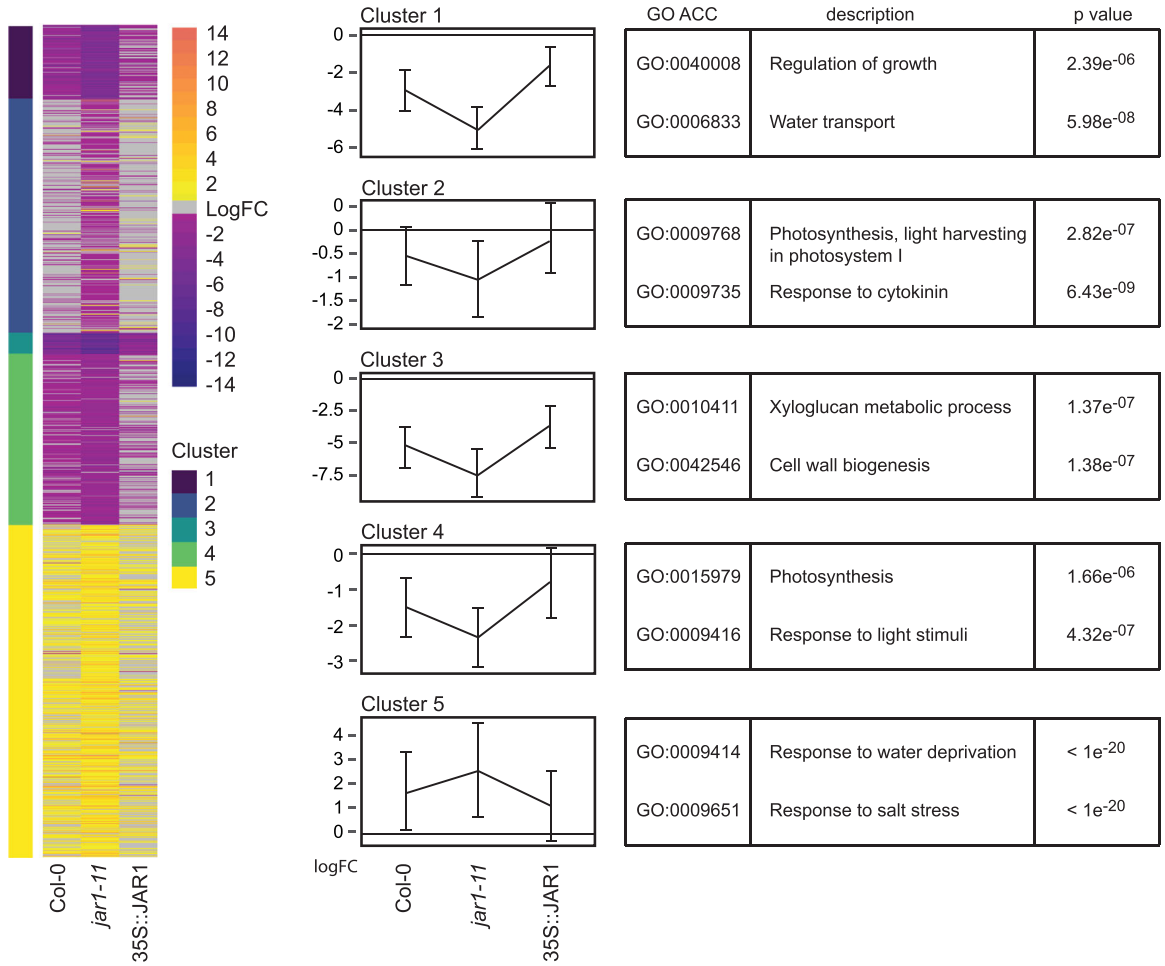


**FIGURE 6** *JASMONATE RESISTANT 1* (*JAR1*)-dependent transcriptomic variations between drought stress and control conditions. Heat map (left) and K-means clustering (middle) of genes up- or down-regulated under drought stress compared with control conditions in the different plant genotypes. K-means clustering analysis was performed to produce the clusters (DESeq, adjusted false discovery rate (FDR) < 0.01 and LogFC ≥ 1) and the thin lines represent the mean expression profiles for each cluster (middle). Only genes that are differentially expressed in at least one of the comparisons were used for the cluster analysis. The top two Gene Ontology (GO) terms for each cluster with *p* are listed (right). [Color figure can be viewed at wileyonlinelibrary.com]

## 3.5 | JAR1-dependent modulation of drought related features and processes

To better explain the different performance of the *jar1-11* and 35S::JAR1 plants under drought, we looked for specific features that would affect water use efficiency. Our RNA-seq analysis had revealed that expression of the two myrosinases (β-thioglucoside glucohydrolases) *TGG1* and *TGG2* was highly elevated in the 35S::JAR1 line under normal growth conditions (Figure 3b and Supporting Information: Data Set S4). These myrosinases were shown to be involved in ABA- and MeJA-induced stomatal closure downstream of ROS production (Islam et al., 2009; Rhaman et al., 2020). In line with this, leaves from 35S::JAR1 plants grown under control conditions displayed a lower stomatal aperture diameter when challenged (Figure 7a). The analysis also revealed a higher stomatal density in *jar1-11* compared with Col-0 and 35S::JAR1 (Figure 7b and Supporting Information: Figure S6), Thus, JAR1-mediated JA-Ile formation affects both the aperture and density of stomata, which together can affect the transpirational water loss.

Flavonoids, such as anthocyanins, have been suggested to scavenge ROS and anthocyanin biosynthesis was shown to be induced by MeJA application (Shan et al., 2009). Accordingly, 35S::JAR1 plants showed higher anthocyanin levels under control conditions compared with Col-0 and *jar1-11* (Figure 7c). In addition, although anthocyanin levels increased significantly in all three plant lines upon drought, the highest increase was observed in 35S::JAR1 plants. Moreover, some genes coding for enzymes involved in GSH synthesis or the ascorbate-GSH cycle were shown to be induced by MeJA application (Sasaki-Sekimoto et al., 2006; Xiang & Oliver, 1998). In our RNA-seq data, very little difference in expression could be observed between Col-0, *jar1-11* and 35S::JAR1 under non-stress conditions (Supporting Information: Data Set S4). However, under drought conditions, differential expression of several genes involved in this process could be observed. Most prominently, *jar1-11* showed

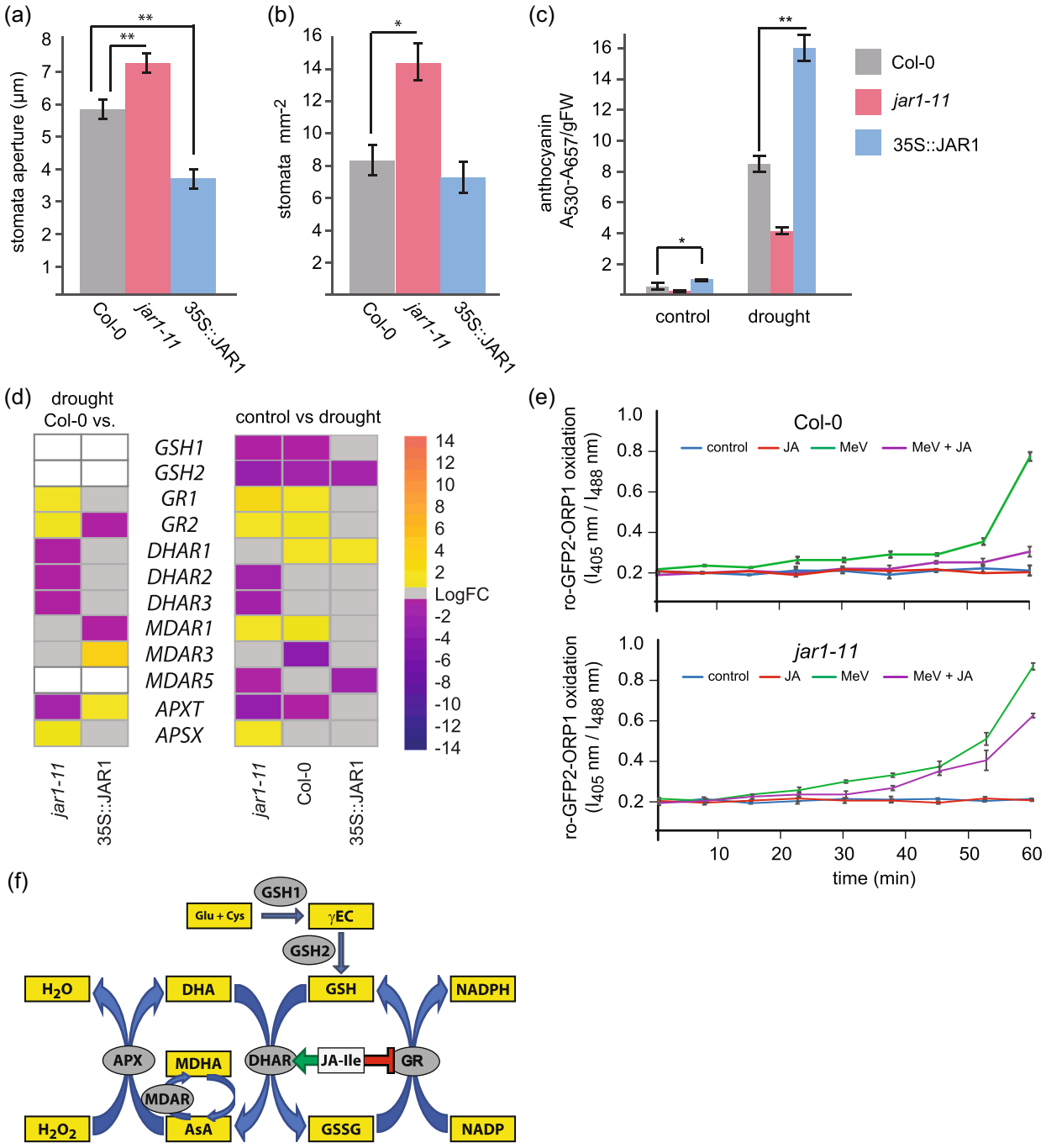


**FIGURE 7** Effect of jasmonoyl-L-isoleucine (JA-Ile) on stomatal regulation, anthocyanin content and MV-induced changes in redox status. Number of stomata (a) and stomatal aperture (b) measured on leaf No. 6 of plants grown under control conditions at Day 21. Data represent means ± SE from three biological replicates ($n = 3$). For stomatal numbers, each replicate quantified leaves from 5 to 6 individual plants. For stomatal aperture, each replicate quantified 90 to 100 stomata in leaves from 6 to 10 individual plants. Data were analysed by one-way analysis of variance (ANOVA) (*$p < 0.05$, **$p < 0.01$) followed by multiple comparisons (Tukey's honest significant difference [HSD] test). (c) Anthocyanin content of different plant genotypes determined in rosette leaves of 32-day-old plants grown under control and drought stress conditions. Data represent means ± SE from three replicates ($n = 3$), each containing three pooled individual plants. Data were analysed by one-way ANOVA (*$p < 0.05$, **$p < 0.01$) followed by multiple comparisons (Tukey's HSD test). (d) Heat maps of differentially expressed genes (DEGs) involved in the ascorbate-glutathione cycle in *jar1-11* and 35S::JAR1 compared with Col-0 under drought conditions (left) or between control and drought conditions in Col-0, *jar1-11* and 35S::JAR1 (right). Data were analysed using a cut-off of false discovery rate (FDR) < 0.05 and LogFC ≥ 0.5. White boxes indicate genes whose changes did not meet the cut-off criteria. (e) Real-time monitoring of redox status using cytosolic roGFP2-Orp1 redox sensors in Col-0 and *jar1-11* leaf cells upon treatment with 10 mM methyl viologen (MeV) and/or 100 µM JA. roGFP2 was excited at wavelengths 405 and 488 nm, and the emission was detected from 505 to 530 nm. Ratios were calculated as the ratiometric image of 405/488 nm. After each run, representative samples were calibrated with 10 mM dithiothreitol (DTT) (ratio = 0.18) and 10 mM $H_2O_2$ (ratio = 1.20). Mean ratios ± SE of different time points represent data from three replicates, each including three individual seedlings. [Color figure can be viewed at wileyonlinelibrary.com]

lower expression of all *DHARs*, the dehydroascorbate reductases that converts GSH to GSSG, and higher expression of *GR1* and *GR2*, GSH reductases that convert GSSG back to GSH (Figure 7d, left panel). Expression of these genes is not much altered in 35S::JAR1 compared with Col-0; however, under drought conditions, the expression of *DHAR1*, the most-highly expressed DHAR isoform, was increased in Col-0 and 35S::JAR1 (Figure 7d, right panel).

To elucidate possible JAR1-mediated effects on ROS scavenging in vivo, we used plants carrying the genetically encoded $H_2O_2$ sensor roGFP-Orp1 (Nietzel et al., 2019). Treatment of leaf tissue from Col-0 plants with 10 mM methyl viologen (MeV), which was shown to lead to oxidative stress and the generation of ROS (Schwarzländer et al., 2009), resulted in a strong oxidative shift of the sensor in both Col-0 and *jar1-11* (Figure 7e, green lines). Application of 100 µM JA, given together with MeV, reduced the MeV-induced increase in $H_2O_2$ levels nearly back to control levels in Col-0 but resulted only in a minor decrease of sensor oxidation in *jar1-11* (Figure 7e, magenta lines). This indicates that JAR1-mediated transformation of JA to JA-Ile is required to reduce MeV-induced ROS and a similar effect would be expected during stress-induced ROS production.

## 4 | DISCUSSION

Plants are constantly exposed to various biotic and abiotic stresses and to combat their detrimental effect, a balance between optimum fitness and resistance mechanism is mandatory. Jasmonate signalling is known to play a role in many developmental and stress-related processes, and in the current work, we used a TDNA insertion mutant in the *JAR1* locus (*jar1-11*) and a novel transgenic line expressing JAR1.1-YFP under the 35 S promoter (35S::JAR1) to alter the endogenous JA-Ile content of *Arabidopsis*. The *jar1-11* mutant showed a strong reduction in *JAR1* transcripts compared with Col-0 (Figure 1a), but a basal level of full-length transcripts is retained despite the disruption of the *JAR1* locus within an exon after about 1/3 of the coding region. It was also shown recently, that a protein encoded by the GH3.10 locus can convert JA to JA-Ile (Delfin et al., 2022). Thus, *jar1-11* is not a null allele, nevertheless, *jar1-11* plants showed a clear reduction in JA-Ile content and nearly null expression of the jasmonate-dependent defence marker *VSP1*, supporting that JAR1 is the major enzyme involved in JA-Ile formation. Moreover, in the 35S::JAR1 line, strongly increased *JAR1* transcript levels result in an about 10-fold increase in JA-Ile content, together with upregulation of *VSP1* and *VSP2*. Thus, these lines are a great resource to study the effects of varying JA-Ile levels on plant growth and stress responses.

### 4.1 | *JAR1* overexpression distorts jasmonate homeostasis

In the *jar1-11* and 35S::JAR1 lines used in this study *JAR1* expression is altered constitutively. Therefore, the effects of altered JAR1 content are already observed under normal growth conditions. Increased content in JA-Ile and its derivatives under these conditions in the 35S::JAR1 lines indicates that JAR1 is not only a key enzyme in jasmonate biosynthesis, but also seems to represent a rate-limiting step of JA-Ile formation (Figure 2). In the wild type, the early onset of drought stress increases *JAR1* expression and thus JA-Ile levels, however, they still remain below that of 35S::JAR1. In *jar1-11*, drought leads to an increase in JA levels, showing that jasmonate synthesis is induced but JA-Ile cannot be produced. However, it is likely that factors other than just the amount of JAR1 protein control JA-Ile levels, especially under drought conditions. As shown here and described before the basal level of the precursor *cis*-OPDA is almost 200 times higher compared with JA-Ile (de Ollas et al., 2015a). Under drought conditions, the level of *cis*-OPDA decreased but still remained much higher than the increased content of JA-Ile. This indicates that JA formation from *cis*-OPDA is not the limiting factor for JA-Ile synthesis. However, the decrease in *cis*-OPDA is at a similar magnitude as the combined increase in JA, JA-Ile and their derivatives, such a 12-OH-JA, 12-OH-JA-Ile and 12-COOH-JA-Ile, all of which accumulate to a greater extent than JA-Ile itself. 12-OH-JA and 12-OH-JA-Ile were both found to modulate JA-Ile-mediated gene expression, including genes involved in jasmonate biosynthesis (Jimenez-Aleman et al., 2019; Poudel et al., 2019). They could thus play a role in balancing JA-Ile homeostasis as well as responses induced by JA-Ile signalling. This fit well with recent findings from Marquis et al. (2022) on the *jao2* mutant, in which changes in JA catabolism affect JA-Ile formation and signalling. Especially intriguing is the general high amount of the JA-derivative 12-*O*-JA-Glc and its further JAR1-dependent increase under drought. 12-*O*-JA-Glc has been shown to accumulate 24 h after wounding of tomato leaves and it was suggested that it also is part of the pathway to remove accumulated JA and JA-Ile under stress (Miersch et al., 2008). Although our study only shows the content of jasmonates at a single (and early) time point during the progressive drought stress, the data strongly support the notion of a continuous flow of JA-Ile synthesis and removal that is enhanced under stress conditions. Constitutive expression of JAR1 distorts this balance, resulting in higher JA-Ile levels.

### 4.2 | Effects of constitutive elevation of JA-Ile on drought resistance and priming

Our study shows that the *jar1-11* mutant (and also *jar1-12*) is more susceptible to progressive drought stress (Figure 4B), whereas 35S::JAR1 plants display only a mild drought stress phenotype. The higher tolerance of 35S::JAR1 is likely based on changes induced by the elevated JA-Ile content. However, JA-Ile content in the 35S::JAR1 line is increased constitutively and not only in response to drought stress. Thus, this resistance could be based on JA-Ile induced changes that happen long before the onset of the drought stress. On the other hand, different JA-Ile levels observed under drought stress could also alter the plant's short term response in a

favourable manner. Indeed, our results indicate that both factors play a role in the better drought resistance of the 35S::JAR1 plants (Supporting Information: Figure S7).

#### 4.2.1 | JAR1-related alterations in plant growth and development

The differences in *JAR1* transcripts and JA-Ile levels in the transgenic lines manifested themselves in opposite phenotypic alterations compared with Col-0 already under non-stress conditions (Figure 1). Overexpression of *JAR1* resulted in shorter and wider leaves, a similar phenotype achieved by treating Col-0 plants with exogenous MeJA application (Figure S5D). This is in agreement with previous findings that MeJA application on *Arabidopsis* seedlings leads to cell cycle arrest, which resulted in reduced leaf growth (Noir et al., 2013; Zhang & Turner, 2008). However, the initial stunted growth observed in 35S::JAR1 seems to be superseded at a later stage by increased radial growth of older leaves. Accordingly, expression of the cell cycle controlling gene *CYCB1.2*, which was found to be down-regulated after exogenous MeJA application in young seedlings (Zhang & Turner, 2008), was upregulated in the older leaves of the 35 S::JAR1 plants used for RNA-seq analysis in our experiments (Supporting Information: Data Set S3). 35S::JAR1 plants also seem to have higher expression levels of the transcriptional co-activator genes *GIF1* and *GRF5* (Supporting Information: Data Set S3), which regulate the development of leaf size and shape (Kim & Kende, 2004; Lee et al., 2009). Mutants in the *GIF1* locus have narrower leaf blades compared with Col-0 indicating that GIF1 regulates lateral leaf expansion. Increased expression of *GIF1* and *GRF5* in 35S::JAR1 could be due to the decreased expression of the *MYC4* TF, which was shown to bind the promoter of *GIF1* and down-regulate its activity (Liu et al., 2020). Reduced leaf growth will reduce the water requirement of the plant and thus can give the 35S::JAR1 plants an advantage under drought conditions.

On the other hand, the *jar1-11* plants show early flowering similar to mutants of the *AOS* and *OPR3* loci that are affected in jasmonate synthesis upstream of JAR1 (Supporting Information: Figure S3C). By contrast, 35S::JAR1 plants flower several days later than *jar1-11* and Col-0 plants. Although there is no difference between the lines with regard to other parameters related to reproductive success (Table S2), a shorter reproductive cycle will likely be of advantage under favourable growth conditions.

#### 4.2.2 | Cross-talk between jasmonate and ABA

Even though MYC2 is considered a master regulator of jasmonate signalling (Dombrecht et al., 2007), it was shown previously that not only JA-Ile but also ABA could induce the expression of *MYC2*. Moreover, the effect of both hormones applied together was much stronger (Lorenzo et al., 2004). This would explain the only slight increase of *MYC2* levels in 35 S::JAR1 under control conditions (Supporting Information: Data Set 3) despite the high level of JA-Ile, because ABA levels are not elevated. Under drought conditions, when ABA levels are high, expression of MYC2 increases in 35S::JAR1 together with genes involved in JA synthesis. This supports a model proposed by Liu et al. (2016), in which exposure to drought activates transcription of *MYC2* via both ABA and jasmonate, which in the form of a positive feedback loop leads to further activation of JA synthesis and subsequently further elevated expression of jasmonate-dependent genes.

Although drought-induced ABA accumulation was evident in all three lines, it was significantly enhanced in *jar1-11* compared with 35S::JAR1 (Figure 2h). Differences in ABA level corresponded to opposite alterations in the expression of genes related to ABA biosynthesis. However, increase in expression of genes related to ABA biosynthesis in *jar-11* was accompanied by upregulation of genes involved in ABA degradation. In addition, *ABI2*, a negative regulator of ABA signalling (Merlot et al., 2001), showed reduced expression in *jar1-11*. A likely explanation is that the *jar1-11* plants evoke mechanisms to attenuate the effects of a surplus in ABA that accumulates in the absence of JA-Ile. This could be one way in which jasmonate signalling helps to keep the balance between drought protection and growth.

#### 4.2.3 | Jasmonate signalling regulates physiological systems involved in drought adaptation and stress response

Better drought resistance of 35S::JAR1 plants likely stems from the relatively high RWC that they retained compared with Col-0, while the loss of RWC was highest in *jar1-11* (Figure 4c). This in turn is a consequence of the variance in stomatal density and stimuli induced stomata closing observed between the plant lines already under non-stress conditions (Figure 7a and Supporting Information: Figure S6). This difference is also in accordance with previous studies showing that exogenously applied MeJA negatively regulates stomatal development and positively regulates stomatal aperture (Han et al., 2018; Hossain et al., 2011). The regulation of stomatal aperture, however, is a very complex process. The higher expression of *TGG1* and *TGG2* in 35S::JAR1 might play a role, since these myrosinases were shown to be involved in ABA- and MeJA-induced stomatal closure downstream of ROS production (Islam et al., 2009). Although plants cannot simply adjust stomata number under drought in fully developed leaves, lesser stomatal aperture of the 35 S::JAR1 plants will attenuate water loss (Supporting Information: Figure S7).

Additionally, 35S::JAR1 plants might cope better with drought stress induced accumulation of $H_2O_2$ and other ROS (Noctor et al., 2014). Controlled redox regulation is important to remove cytotoxic ROS levels, while sustaining ROS-dependent regulatory circuits. We could show that external addition of JA alleviates MeV-induced $H_2O_2$ production in Col-0 but not in the *jar1-11* mutant (Figure 7d), where JA cannot be converted into JA-Ile. Previously, external MeJA application was reported to induce some genes involved in the

ascorbate-GSH cycle, one of the major mechanisms to adjust cytosolic $H_2O_2$ levels (Sasaki-Sekimoto et al., 2006; Xiang & Oliver, 1998). In our study, we observed upregulation of both *DHAR1* and *GR1* under drought in Col-0. DHAR and GR are responsible for the conversion of GSH to GSSSG and back, respectively, a central reaction of the ascorbate-GSH cycle (Figure 7e). We did not see any difference in the expression of ascorbate-GSH cyclegenes under non-stress conditions in 35S::JAR1, despite the increase in JA-Ile levels. However, *DHAR1* and *GR1/2* expression was differential regulated in *jar1-11* and 35S::JAR1 under drought. Together, our data suggest that rather than generally inducing its activity, JA-Ile might adjust the flow through the ascorbate-GSH cycle under drought conditions.

### 4.3 | JA-Ile-mediated global transcriptome changes

Cluster analysis of the RNA-seq data identified hubs of altered gene expression between *jar1-11*, Col-0 and 35S::JAR1 under drought conditions. Many of these fall into categories that can be easily related to drought responses, such as photosynthesis and water transport, or they represent known genes related to drought or general stress. For each of these individual genes and clusters subsequent studies will have to show whether their expression is directly altered by JA-Ile and they are thus involved in jasmonate-related drought susceptibility and tolerance. Changes in their expression could also be a manifestation of the different drought phenotypes and thus an indirect effect. In this context, it should be noted that even under control conditions, 35S::JAR1 plants showed downregulation of certain drought (*RD29A*, *ERD7*, *LEA14* and *GCR2*) and cold-responsive (*COR15B)* genes; however, further studies have to show whether this has an effect of the observed drought resistance of these plants.

Overall, our data show that constitutive deregulation of jasmonate homeostasis provides *Arabidopsis* with better drought resistance. They provide insight into the effects that changes in JA-Ile content have on various morphological and physiological traits that can be related to drought. The results further indicate that priming, that is, changes happening long before the onset of the drought stress, as well as direct stress responses both shape the drought resistance of 35S::JAR1 (Supporting Information: Figure S7). These findings are in line with results from Marquis and coworkers (Marquis et al., 2022) showing that modulating JA turnover improved the resistance of *Arabidopsis* to drought and that the drought tolerance of the *jao2* mutant requires JA-Ile formation by JAR1. Thus, constitutively altering jasmonate homeostasis can be a way to adapt plants to better withstand drought but possible detrimental variations in growth and life-cycle length under more favourable conditions have to be considered.

## ACKNOWLEDGMENTS

We gratefully acknowledge funding by the Deutscher Akademischer Austauschdienst (DAAD) to Sakil Mahmud (grant number 57299294) and by the Deutsche Forschungsgemeinschaft (DFG) to Annika Kortz (grant number 397753445), Ute C. Vothknecht (INST 217/939-1 FUGG) and Peng Yu (Emmy Noether Programme, grant number 444755415). We are grateful to Professor Dr. Frank Hochholdinger, INRES, Crop Functional Genomics, University of Bonn, for facilitating the RNA-seq data analysis in his group. We acknowledge the NGS Core Facility, University of Bonn, for providing the RNA-seq service. Finally, we thank Dr. Fatima Chigri for careful proofreading of the manuscript. We also thank Dr. Stefanie Müller-Schüssele for assistance with the roGFP2-ORP1 measurements, Professor Markus Schwärzlander, University of Münster, for providing roGFP2-Orp1 seeds, and Diego Clavijo for assistance with plant growth. Open Access funding enabled and organized by Projekt DEAL.

## CONFLICT OF INTEREST

The authors declare no conflict of interest.

## ORCID

*Chhana Ullah* http://orcid.org/0000-0002-8898-669X
*Ute C. Vothknecht* http://orcid.org/0000-0002-8930-0127

## REFERENCES

Barrs, H.D. & Weatherley, P.E. (1962) A re-examination of relative turgidity technique for estimating water deficits in leaves. *Australian Journal of Biological Sciences*, 15(3), 413–428. https://doi.org/10.1071/Bi9620413

Bell, E., Creelman, R.A. & Mullet, J.E. (1995) A chloroplast lipoxygenase is required for wound-induced jasmonic acid accumulation in *Arabidopsis*. *Proceedings of the National Academy of Sciences of the United States of America*, 92(19), 8675–8679. https://doi.org/10.1073/pnas.92.19.8675

Bhosale, R., Jewell, J.B., Hollunder, J., Koo, A.J., Vuylsteke, M. & Michoel, T. et al. (2013) Predicting gene function from uncontrolled expression variation among individual wild-type *Arabidopsis* plants. *The Plant Cell*, 25(8), 2865–2877. https://doi.org/10.1105/tpc.113.112268

Capella, A.N., Menossi, M., Arruda, P. & Benedetti, C.E. (2001) COI1 affects myrosinase activity and controls the expression of two flower-specific myrosinase-binding protein homologues in *Arabidopsis*. *Planta*, 213(5), 691–699. https://doi.org/10.1007/s004250100548

Cheng, C.Y., Krishnakumar, V., Chan, A.P., Thibaud-Nissen, F., Schobel, S. & Town, C.D. (2017) Araport11: a complete reannotation of the *Arabidopsis thaliana* reference genome. *Plant Journal*, 89(4), 789–804. https://doi.org/10.1111/tpj.13415

Core Team, R. (2020) *R: a language and environment for statistical computing*. R Foundation for Statistical Computing. www.R-project.org

Creelman, R.A. & Mullet, J.E. (1995) Jasmonic acid distribution and action in plants: regulation during development and response to biotic and abiotic stress. *Proceedings of the National Academy of Sciences of the United States of America*, 92(10), 4114–4119. https://doi.org/10.1073/pnas.92.10.4114

Datla, R.S., Hammerlindl, J.K., Panchuk, B., Pelcher, L.E. & Keller, W. (1992) Modified binary plant transformation vectors with the wild-type gene encoding NPTII. *Gene*, 122(2), 383–384. https://doi.org/10.1016/0378-1119(92)90232-e

Delfin, J.C., Kanno, Y., Seo, M., Kitaoka, N., Matsuura, H., Tohge, T. et al. (2022) AtGH3.10 is another jasmonic acid-amido synthetase in *Arabidopsis thaliana*. *Plant Journal*, 110(4), 1082–1096. https://doi.org/10.1111/tpj.15724

Devoto, A., Ellis, C., Magusin, A., Chang, H.S., Chilcott, C., Zhu, T. et al. (2005) Expression profiling reveals COI1 to be a key regulator of

genes involved in wound- and methyl jasmonate-induced secondary metabolism, defence, and hormone interactions. *Plant Molecular Biology*, 58(4), 497–513. https://doi.org/10.1007/s11103-005-7306-5

Dombrecht, B., Xue, G.P., Sprague, S.J., Kirkegaard, J.A., Ross, J.J., Reid, J.B. et al. (2007) MYC2 differentially modulates diverse jasmonate-dependent functions in *Arabidopsis*. *The Plant Cell*, 19(7), 2225–2245. https://doi.org/10.1105/tpc.106.048017

Du, H., Liu, H. & Xiong, L. (2013) Endogenous auxin and jasmonic acid levels are differentially modulated by abiotic stresses in rice. *Frontiers in Plant Science*, 4, 397. https://doi.org/10.3389/fpls.2013.00397

Fernández-Calvo, P., Chini, A., Fernández-Barbero, G., Chico, J.M., Gimenez-Ibanez, S., Geerinck, J. et al. (2011) The *Arabidopsis* bHLH transcription factors MYC3 and MYC4 are targets of JAZ repressors and act additively with MYC2 in the activation of Jasmonate responses. *The Plant Cell*, 23(2), 701–715. https://doi.org/10.1105/tpc.110.080788

Gao, X.P., Wang, X.F., Lu, Y.F., Zhang, L.Y., Shen, Y.Y., Liang, Z. et al. (2004) Jasmonic acid is involved in the water-stress-induced betaine accumulation in pear leaves. *Plant, Cell and Environment*, 27(4), 497–507. https://doi.org/10.1111/j.1365-3040.2004.01167.x

Han, X., Hu, Y.R., Zhang, G.S., Jiang, Y.J., Chen, X.L. & Yu, D.Q. (2018) Jasmonate negatively regulates stomatal development in *Arabidopsis* cotyledons. *Plant Physiology*, 176(4), 2871–2885. https://doi.org/10.1104/pp.17.00444

Harb, A., Krishnan, A., Ambavaram, M.M. & Pereira, A. (2010) Molecular and physiological analysis of drought stress in *Arabidopsis* reveals early responses leading to acclimation in plant growth. *Plant Physiology*, 154(3), 1254–1271. https://doi.org/10.1104/pp.110.161752

Hickman, R., Van Verk, M.C., Van Dijken, A., Mendes, M.P., Vroegop-Vos, I.A., Caarls, L. et al. (2017) Architecture and dynamics of the jasmonic acid gene regulatory network. *The Plant Cell*, 29(9), 2086–2105. https://doi.org/10.1105/tpc.16.00958

Hossain, M.A., Munemasa, S., Uraji, M., Nakamura, Y., Mori, I.C. & Murata, Y. (2011) Involvement of endogenous abscisic acid in methyl Jasmonate-induced stomatal closure in *Arabidopsis*. *Plant Physiology*, 156(1), 430–438. https://doi.org/10.1104/pp.111.172254

Islam, M.M., Tani, C., Watanabe-Sugimoto, M., Uraji, M., Jahan, M.S., Masuda, C. et al. (2009) Myrosinases, TGG1 and TGG2, redundantly function in ABA and MeJA signaling in *Arabidopsis* guard cells. *Plant and Cell Physiology*, 50(6), 1171–1175. https://doi.org/10.1093/pcp/pcp066

Jimenez-Aleman, G.H., Almeida-Trapp, M., Fernández-Barbero, G., Gimenez-Ibanez, S., Reichelt, M., Vadassery, J. et al. (2019) Omega hydroxylated JA-Ile is an endogenous bioactive jasmonate that signals through the canonical jasmonate signaling pathway. *Biochimica Et Biophysica Acta-Molecular and Cell Biology of Lipids*, 1864(12), 158520. https://doi.org/10.1016/j.bbalip.2019.158520

Kim, J.H. & Kende, H. (2004) A transcriptional coactivator, AtGIF1, is involved in regulating leaf growth and morphology in *Arabidopsis*. *Proceedings of the National Academy of Sciences of the United States of America*, 101(36), 13374–13379. https://doi.org/10.1073/pnas.0405450101

Kinoshita, A. & Richter, R. (2020) Genetic and molecular basis of floral induction in *Arabidopsis thaliana*. *Journal of Experimental Botany*, 71(9), 2490–2504. https://doi.org/10.1093/jxb/eraa057

Koo, A.J. (2018) Metabolism of the plant hormone jasmonate: a sentinel for tissue damage and master regulator of stress response. *Phytochemistry Reviews*, 17(1), 51–80. https://doi.org/10.1007/s11101-017-9510-8

Lee, B.H., Ko, J.H., Lee, S., Lee, Y., Pak, J.H. & Kim, J.H. (2009) The *Arabidopsis* GRF-INTERACTING FACTOR gene family performs an overlapping function in determining organ size as well as multiple developmental properties. *Plant Physiology*, 151(2), 655–668. https://doi.org/10.1104/pp.109.141838

Liu, N., Staswick, P.E. & Avramova, Z. (2016) Memory responses of jasmonic acid-associated *Arabidopsis* genes to a repeated dehydration stress. *Plant, Cell and Environment*, 39(11), 2515–2529. https://doi.org/10.1111/pce.12806

Liu, Y., Du, M., Deng, L., Shen, J., Fang, M. & Chen, Q. et al. (2019) MYC2 regulates the termination of jasmonate signaling via an autoregulatory negative feedback loop. *The Plant Cell*, 31(1), 106–127. https://doi.org/10.1105/tpc.18.00405

Liu, Z.P., Li, N., Zhang, Y.Y. & Li, Y.H. (2020) Transcriptional repression of GIF1 by the KIX-PPD-MYC repressor complex controls seed size in *Arabidopsis*. *Nature Communications*, 11(1), 1846. https://doi.org/10.1038/s41467-020-15603-3

Lorenzo, O., Chico, J.M., Sanchez-Serrano, J.J. & Solano, R. (2004) Jasmonate-insensitive1 encodes a MYC transcription factor essential to discriminate between different jasmonate-regulated defense responses in *Arabidopsis*. *The Plant Cell*, 16(7), 1938–1950. https://doi.org/10.1105/tpc.022319

Marquis, V., Smirnova, E., Graindorge, S., Delcros, P., Villette, C., Zumsteg, J. et al. (2022) Broad-spectrum stress tolerance conferred by suppressing jasmonate signaling attenuation in *Arabidopsis* JASMONIC ACID OXIDASE mutants. *The Plant Journal*, 109(4), 856–872. https://doi.org/10.1111/tpj.15598

Merlot, S., Gosti, F., Guerrier, D., Vavasseur, A. & Giraudat, J. (2001) The ABI1 and ABI2 protein phosphatases 2C act in a negative feedback regulatory loop of the abscisic acid signalling pathway. *Plant Journal*, 25(3), 295–303. https://doi.org/10.1046/j.1365-313x.2001.00965.x

Meyer, A. J., Brach, T., Marty, L., Kreye, S., Rouhier, N., Jacquot, J. P., & Hell, R. (2007). Redox-sensitive GFP in Arabidopsis thaliana is a quantitative biosensor for the redox potential of the cellular glutathione redox buffer. *Plant Journal*, 52(5), 973–986. https://doi.org/10.1111/j.1365-313X.2007.03280.x

Michaels, S.D. & Amasino, R.M. (2001) Loss of FLOWERING LOCUS C activity eliminates the late-flowering phenotype of FRIGIDA and autonomous pathway mutations but not responsiveness to vernalization. *The Plant Cell*, 13(4), 935–941. https://doi.org/10.1105/tpc.13.4.935

Miersch, O., Neumerkel, J., Dippe, M., Stenzel, I. & Wasternack, C. (2008) Hydroxylated jasmonates are commonly occurring metabolites of jasmonic acid and contribute to a partial switch-off in jasmonate signaling. *New Phytologist*, 177(1), 114–127. https://doi.org/10.1111/j.1469-8137.2007.02252.x

Nietzel, T., Elsässer, M., Ruberti, C., Steinbeck, J., Ugalde, J.M., Fuchs, P. et al. (2019) The fluorescent protein sensor roGFP2-Orp1 monitors in vivo H2O2 and thiol redox integration and elucidates intracellular H2O2 dynamics during elicitor-induced oxidative burst in *Arabidopsis*. *New Phytologist*, 221(3), 1649–1664. https://doi.org/10.1111/nph.15550

Noctor, G., Mhamdi, A. & Foyer, C.H. (2014) The roles of reactive oxygen metabolism in drought: not so cut and dried. *Plant Physiology*, 164(4), 1636–1648. https://doi.org/10.1104/pp.113.233478

Noir, S., Bömer, M., Takahashi, N., Ishida, T., Tsui, T.L., Balbi, V. et al. (2013) Jasmonate controls leaf growth by repressing cell proliferation and the onset of endoreduplication while maintaining a potential stand-by mode. *Plant Physiology*, 161(4), 1930–1951. https://doi.org/10.1104/pp.113.214908

de Ollas, C., Arbona, V. & Gomez-Cadenas, A. (2015a) Jasmonic acid interacts with abscisic acid to regulate plant responses to water stress conditions. *Plant Signaling & Behavior*, 10(12), e1078953. https://doi.org/10.1080/15592324.2015.1078953

de Ollas, C., Arbona, V. & Gomez-Cadenas, A. (2015b) Jasmonoyl isoleucine accumulation is needed for abscisic acid build-up in roots of *Arabidopsis* under water stress conditions. *Plant, Cell and Environment*, 38(10), 2157–2170. https://doi.org/10.1111/pce.12536

Poudel, A.N., Holtsclaw, R.E., Kimberlin, A., Sen, S., Zeng, S., Joshi, T. et al. (2019) 12-Hydroxy-Jasmonoyl-l-Isoleucine is an active jasmonate that signals through CORONATINE INSENSITIVE 1 and contributes to the wound response in *Arabidopsis*. *Plant and Cell Physiology*, 60(10), 2152–2166. https://doi.org/10.1093/pcp/pcz109

Ratcliffe, O.J., Nadzan, G.C., Reuber, T.L. & Riechmann, J.L. (2001) Regulation of flowering in *Arabidopsis* by an FLC homologue. *Plant Physiology*, 126(1), 122–132. https://doi.org/10.1104/pp.126.1.122

Rhaman, M.S., Nakamura, T., Nakamura, Y., Munemasa, S. & Murata, Y. (2020) The myrosinases TGG1 and TGG2 function redundantly in reactive carbonyl species signaling in *Arabidopsis* guard cells. *Plant and Cell Physiology*, 61(5), 967–977. https://doi.org/10.1093/pcp/pcaa024

Sasaki-Sekimoto, Y., Taki, N., Obayashi, T., Aono, M., Matsumoto, F. & Sakurai, N. et al. (2006) Coordinated activation of metabolic pathways for antioxidants and defence compounds by jasmonates and their roles in stress tolerance in *Arabidopsis*. *Plant and Cell Physiology*, 47, S233.

Savchenko, T.V., Rolletschek, H. & Dehesh, K. (2019) Jasmonates-mediated rewiring of central metabolism regulates adaptive responses. *Plant and Cell Physiology*, 60(12), 2613–2620. https://doi.org/10.1093/pcp/pcz181

Schwarzländer, M., Fricker, M.D. & Sweetlove, L.J. (2009) Monitoring the in vivo redox state of plant mitochondria: effect of respiratory inhibitors, abiotic stress and assessment of recovery from oxidative challenge. *Biochimica Et Biophysica Acta-Bioenergetics*, 1787(5), 468–475. https://doi.org/10.1016/j.bbabio.2009.01.020

Shan, X.Y., Zhang, Y.S., Peng, W., Wang, Z.L. & Xie, D.X. (2009) Molecular mechanism for jasmonate-induction of anthocyanin accumulation in *Arabidopsis*. *Journal of Experimental Botany*, 60(13), 3849–3860. https://doi.org/10.1093/jxb/erp223

Smirnova, E., Marquis, V., Poirier, L., Aubert, Y., Zumsteg, J., Ménard, R. et al. (2017) Jasmonic acid oxidase 2 hydroxylates jasmonic acid and represses basal defense and resistance responses against *Botrytis cinerea* infection. *Molecular Plant*, 10(9), 1159–1173. https://doi.org/10.1016/j.molp.2017.07.010

Staswick, P.E. & Tiryaki, I. (2004) The oxylipin signal jasmonic acid is activated by an enzyme that conjugates it to isoleucine in *Arabidopsis*. *The Plant Cell*, 16(8), 2117–2127. https://doi.org/10.1105/tpc.104.023549

Suza, W.P. & Staswick, P.E. (2008) The role of JAR1 in Jasmonoyl-L-isoleucine production during *Arabidopsis* wound response. *Planta*, 227(6), 1221–1232. https://doi.org/10.1007/s00425-008-0694-4

Tayyab, N., Naz, R., Yasmin, H., Nosheen, A., Keyani, R., Sajjad, M. et al. (2020) Combined seed and foliar pre-treatments with exogenous methyl jasmonate and salicylic acid mitigate drought-induced stress in maize. *PLoS One*, 15(5), e0232269. https://doi.org/10.1371/journal.pone.0232269

Tukey, H.B. & Hamner, C.L. (1949) Form and composition of cherry fruits (Prunus-Avium and P-Cerasus) following fall applications of 2,4-Dichlorophenoxyacetic acid and naphthalene acetic acid. *Proceedings of the American Society for Horticultural Science*, 54(Dec), 95–101.

Ullah, C., Schmidt, A., Reichelt, M., Tsai, C.-J. & Gershenzon, J. (2022) Lack of antagonism between salicylic acid and jasmonate signalling pathways in poplar. *New Phytologist*, 235(2), 701–717.

Ullah, C., Tsai, C.J., Unsicker, S.B., Xue, L., Reichelt, M., Gershenzon, J. et al. (2019) Salicylic acid activates poplar defense against the biotrophic rust fungus *Melampsora larici-populina* via increased biosynthesis of catechin and proanthocyanidins. *New Phytologist*, 221(2), 960–975.

Vercruysse, J., Baekelandt, A., Gonzalez, N. & Inzé, D. (2020) Molecular networks regulating cell division during *Arabidopsis* leaf growth. *Journal of Experimental Botany*, 71(8), 2365–2378. https://doi.org/10.1093/jxb/erz522

Wang, X., Li, Q., Xie, J., Huang, M., Cai, J. & Zhou, Q. et al. (2021) Abscisic acid and jasmonic acid are involved in drought priming-induced tolerance to drought in wheat. *Crop Journal*, 9(1), 120–132. https://doi.org/10.1016/j.cj.2020.06.002

Wasternack, C. & Song, S.S. (2017) Jasmonates: biosynthesis, metabolism, and signaling by proteins activating and repressing transcription. *Journal of Experimental Botany*, 68(6), 1303–1321. https://doi.org/10.1093/jxb/erw443

Widemann, E., Miesch, L., Lugan, R., Holder, E., Heinrich, C., Aubert, Y. et al. (2013) The amidohydrolases IAR3 and ILL6 contribute to Jasmonoyl-Isoleucine hormone turnover and generate 12-Hydroxyjasmonic acid upon wounding in *Arabidopsis* leaves. *Journal of Biological Chemistry*, 288(44), 31701–31714. https://doi.org/10.1074/jbc.M113.499228

Wu, G., & Poethig, R.S. (2006). Temporal regulation of shoot development in Arabidopsis thalianaby miR156 and its target SPL3. *Development*, 133(18), 3539–3547. https:/doi.org/10.1242/dev.02521

Wu, Z., Fang, X., Zhu, D. & Dean, C. (2020) Autonomous pathway: FLOWERING LOCUS C repression through an antisense-mediated chromatin-silencing mechanism1 [CC-BY]. *Plant Physiology*, 182(1), 27–37. https://doi.org/10.1104/pp.19.01009

Xiang, C.B. & Oliver, D.J. (1998) Glutathione metabolic genes coordinately respond to heavy metals and jasmonic acid in *Arabidopsis*. *The Plant Cell*, 10(9), 1539–1550. https://doi.org/10.1105/tpc.10.9.1539

Yang, S., Vanderbeld, B., Wan, J. & Huang, Y. (2010) Narrowing down the targets: towards successful genetic engineering of drought-tolerant crops. *Molecular Plant*, 3(3), 469–490. https://doi.org/10.1093/mp/ssq016

Zander, M., Lewsey, M.G., Clark, N.M., Yin, L., Bartlett, A., Saldierna Guzmán, J.P. et al. (2020) Integrated multi-omics framework of the plant response to jasmonic acid. *Nature Plants*, 6(3), 290–302. https://doi.org/10.1038/s41477-020-0605-7

Zhang, Y. & Turner, J.G. (2008) Wound-induced endogenous jasmonates stunt plant growth by inhibiting mitosis. *PLoS One*, 3(11), e3699. https://doi.org/10.1371/journal.pone.0003699

Züst, T. & Agrawal, A.A. (2017) Trade-offs between plant growth and defense against insect herbivory: an emerging mechanistic synthesis. *Annual Review of Plant Biology*, 68, 513–534. https://doi.org/10.1146/annurev-arplant-042916-040856

## SUPPORTING INFORMATION

Additional supporting information can be found online in the Supporting Information section at the end of this article.

**How to cite this article:** Mahmud, S., Ullah, C., Kortz, A., Bhattacharyya, S., Yu, P., Gershenzon, J., et al. (2022) Constitutive expression of *JASMONATE RESISTANT 1* induces molecular changes that prime the plants to better withstand drought. *Plant, Cell & Environment*, 1–17. https://doi.org/10.1111/pce.14402